

Acta Crystallographica Section E

Structure Reports

Online

ISSN 1600-5368

Pirquitasite, $\text{Ag}_2\text{ZnSnS}_4$ Benjamin N. Schumer,^{a*} Robert T. Downs,^a Kenneth J. Domanik,^b Marcelo B Andrade^a and Marcus J. Origlieri^a^aDepartment of Geosciences, University of Arizona, Tucson, Arizona 85721-0077, USA, and ^bLunar and Planetary Laboratory, University of Arizona, 1629 E. University Boulevard, Tucson, AZ 85721-0092, USA

Correspondence e-mail: bschumer@email.arizona.edu

Received 19 December 2012; accepted 10 January 2013

Key indicators: single-crystal X-ray study; $T = 293$ K; mean $\sigma(\text{Sn}-\text{S}) = 0.002$ Å; disorder in main residue; R factor = 0.027; wR factor = 0.070; data-to-parameter ratio = 24.0.

Pirquitasite, ideally $\text{Ag}_2\text{ZnSnS}_4$ (disilver zinc tin tetrasulfide), exhibits tetragonal symmetry and is a member of the stannite group that has the general formula A_2BCX_4 , with $A = \text{Ag}, \text{Cu}$; $B = \text{Zn}, \text{Cd}, \text{Fe}, \text{Cu}, \text{Hg}$; $C = \text{Sn}, \text{Ge}, \text{Sb}, \text{As}$; and $X = \text{S}, \text{Se}$. In this study, single-crystal X-ray diffraction data are used to determine the structure of pirquitasite from a twinned crystal from the type locality, the Pirquitas deposit, Jujuy Province, Argentina, with anisotropic displacement parameters for all atoms, and a measured composition of $(\text{Ag}_{1.87}\text{Cu}_{0.13})(\text{Zn}_{0.61}\text{Fe}_{0.36}\text{Cd}_{0.03})\text{SnS}_4$. One Ag atom is located on Wyckoff site Wyckoff $2a$ (symmetry $\bar{4}$.), the other Ag atom is statistically disordered with minor amounts of Cu and is located on $2c$ ($\bar{4}$.), the (Zn, Fe, Cd) site on $2d$ ($\bar{4}$.), Sn on $2b$ ($\bar{4}$.), and S on general site $8g$. This is the first determination of the crystal structure of pirquitasite, and our data indicate that the space group of pirquitasite is $\bar{4}$, rather than $\bar{4}2m$ as previously suggested. The structure was refined under consideration of twinning by inversion [twin ratio of the components 0.91 (6):0.09 (6)].

Related literature

For related structures in the stannite–kesterite series, see: Orlova (1956); Hall *et al.* (1978); Kissin & Owens (1979); Bonazzi *et al.* (2003). For previous work on hocartite and pirquitasite, see: Johan & Picot (1982). For details on synthetic stannite group phases, see: Salomé *et al.* (2012); Sasamura *et al.* (2012); Tsuji *et al.* (2010). For other stannite group minerals, see: Chen *et al.* (1998); Frenzel (1959); Garin & Parthé (1972); Johan *et al.* (1971); Kaplunnik *et al.* (1977); Kissin & Owens (1989); Marumo & Nowaki (1967); Murciego *et al.* (1999); Szymański (1978); Wintenberger (1979).

Experimental

Crystal data

$(\text{Ag}_{1.87}\text{Cu}_{0.13})(\text{Zn}_{0.61}\text{Fe}_{0.36}\text{Cd}_{0.03})\text{SnS}_4$
 $M_r = 520.26$
 Tetragonal, $\bar{4}$
 $a = 5.7757$ (12) Å
 $c = 10.870$ (2) Å

$V = 362.60$ (13) Å³
 $Z = 2$
 Mo $K\alpha$ radiation
 $\mu = 12.58$ mm⁻¹
 $T = 293$ K
 $0.05 \times 0.05 \times 0.04$ mm

Data collection

Bruker APEXII CCD area-detector diffractometer
 Absorption correction: multi-scan (*SADABS*; Sheldrick, 2005)
 $T_{\min} = 0.572$, $T_{\max} = 0.633$
 1312 measured reflections
 575 independent reflections
 570 reflections with $I > 2\sigma(I)$
 $R_{\text{int}} = 0.013$

Refinement

$R[F^2 > 2\sigma(F^2)] = 0.027$
 $wR(F^2) = 0.070$
 $S = 1.17$
 575 reflections
 24 parameters
 4 restraints
 $\Delta\rho_{\text{max}} = 1.05$ e Å⁻³
 $\Delta\rho_{\text{min}} = -0.87$ e Å⁻³
 Absolute structure: Flack (1983)
 Flack parameter: 0.91 (6)

Table 1

Table 1. Minerals of the Stannite Group.

Mineral	Formula	Space Group	Reference
Stannite	$\text{Cu}_2\text{FeSnS}_4$	$\bar{4}2m$	Hall <i>et al.</i> (1978)
Hocartite	$\text{Ag}_2\text{FeSnS}_4$	$\bar{4}2m$	Johan & Picot (1982)
Kuramite	$\text{Cu}_2^{1+}\text{Cu}^{2+}\text{SnS}_4$	$\bar{4}2m$	Chen <i>et al.</i> (1998)
Černyite	$\text{Cu}_2\text{CdSnS}_4$	$\bar{4}2m$	Szymański (1978)
Velikite	$\text{Cu}_2\text{HgSnS}_4$	$\bar{4}2m$	Kaplunnik <i>et al.</i> (1977)
Famatinitite	$\text{Cu}_2^{1+}\text{Cu}^{2+}\text{SbS}_4$	$\bar{4}2m$	Garin & Parthé (1972)
Luzonite	$\text{Cu}_2^{1+}\text{Cu}^{2+}\text{AsS}_4$	$\bar{4}2m$	Marumo & Nowaki (1967)
Barquillite	$\text{Cu}_2(\text{Cd}, \text{Fe}^{2+})\text{GeS}_4$	$\bar{4}2m$	Murciego <i>et al.</i> (1999)
Briartite	$\text{Cu}_2\text{FeGeS}_4$	$\bar{4}2m$	Wintenberger (1979)
Permingeatite	$\text{Cu}_2^{1+}\text{Cu}^{2+}\text{SbSe}_4$	$\bar{4}2m$	Johan <i>et al.</i> (1971)
Kesterite	$\text{Cu}_2\text{ZnSnS}_4$	$\bar{4}$	Kissin & Owens (1979)
Ferrokesterite	$\text{Cu}_2(\text{Fe}, \text{Zn})\text{SnS}_4$	$\bar{4}$	Kissin & Owens (1989)
Pirquitasite	$\text{Ag}_2\text{ZnSnS}_4$	$\bar{4}$	This study
Idaite	$\text{Cu}_2^+\text{Cu}^{2+}\text{FeS}_4$	Unknown	Frenzel (1959)

Data collection: *APEX2* (Bruker, 2004); cell refinement: *SAINT* (Bruker, 2004); data reduction: *SAINT*; program(s) used to solve structure: *SHELXS97* (Sheldrick, 2008); program(s) used to refine structure: *SHELXL97* (Sheldrick, 2008); molecular graphics: *Xtal-Draw* (Downs & Hall-Wallace, 2003); software used to prepare material for publication: *publCIF* (Westrip, 2010).

We gratefully acknowledge the support of the Arizona Science Foundation and CNPq 202469/2011–5 from the Brazilian Government for MBA. Special thanks go to Dr David Brown for pointing out that bond-valence calculations corroborate the ordering of Cu to the Ag₂ site.

Supplementary data and figures for this paper are available from the IUCr electronic archives (Reference: BR2219).

References

- Bonazzi, P., Bindi, L., Bernardini, G. P. & Menchetti, S. (2003). *Can. Mineral.* **41**, 639–647.
- Bruker (2004). *APEX2* and *SAINT*. Bruker AXS Inc., Madison, Wisconsin, USA.
- Chen, X., Wada, H., Sato, A. & Mieno, M. (1998). *J. Appl. Chem.* **139**, 144–151.
- Downs, R. T. & Hall-Wallace, M. (2003). *Am. Mineral.* **88**, 247–250.
- Flack, H. D. (1983). *Acta Cryst.* **A39**, 876–881.
- Frenzel, G. (1959). *N. Jahrb. Min. Abh.* **93**, 87–114.
- Garin, J. & Parthé, E. (1972). *Acta Cryst.* **B28**, 3672–3674.
- Hall, S. R., Szymański, J. T. & Stewart, J. M. (1978). *Can. Mineral.* **16**, 131–137.
- Johan, Z. & Picot, P. (1982). *Bull. Mineral.* **105**, 229–235.
- Johan, Z., Picot, P., Pierrot, R. & Kvacek, M. (1971). *Bull. Soc. Fr. Min. Cryst.* **94**, 162–165.
- Kaplunnik, L. N., Pobedinskaya, B. A. & Belov, N. V. (1977). *Sov. Phys. Crystallogr.* **22**, 99–100.
- Kissin, S. A. & Owens, D. R. (1979). *Can. Mineral.* **17**, 125–135.
- Kissin, S. A. & Owens, D. R. (1989). *Can. Mineral.* **27**, 673–688.
- Marumo, F. & Nowaki, W. (1967). *Z. Kristallogr.* **124**, 1–8.
- Murciego, A., Pascua, M. I., Babkine, J., Dusausoy, Y., Medenbach, O. & Bernhardt, H. J. (1999). *Eur. J. Mineral.* **11**, 111–117.
- Orlova, Z. V. (1956). *Trudy Vses. Mag. Nauch.* **2**, 76–84.
- Salomé, P. M. P., Malaquais, J., Fernandes, P. A., Ferreira, M. S., da Cunha, A. F., Leitão, J. P., Gonzales, J. C. & Matinaga, F. M. (2012). *Solar En. Mat. Solar Cells*, **101**, 147–153.
- Sasamura, T., Osaki, T., Kameyama, T., Shibayama, T., Kudo, A., Kuwobata, S. & Torimoto, T. (2012). *Chem. Lett.* **41**, 1009–1011.
- Sheldrick, G. M. (2005). *SADABS*. University of Göttingen, Germany.
- Sheldrick, G. M. (2008). *Acta Cryst.* **A64**, 112–122.
- Szymański, J. T. (1978). *Can. Mineral.* **16**, 147–151.
- Tsuji, I., Shimodaira, Y., Kato, H., Kobayashi, H. & Kudo, A. (2010). *Chem. Mater.* **22**, 1402–1409.
- Westrip, S. P. (2010). *J. Appl. Cryst.* **43**, 920–925.
- Wintenberger, M. (1979). *Mat. Res. Bull.* **14**, 1195–1202.

supplementary materials

Acta Cryst. (2013). E69, i8–i9 [doi:10.1107/S1600536813001013]

Pirquitasite, $\text{Ag}_2\text{ZnSnS}_4$

Benjamin N. Schumer, Robert T. Downs, Kenneth J. Domanik, Marcelo B Andrade and Marcus J. Origlieri

Comment

Pirquitasite is a member of the stannite group of tetragonal sulfides, which exhibit space group $\bar{I}4_2m$ or $\bar{I}4$, and is an ordered derivative of the sphalerite structure (Johan and Picot, 1982). The stannite group currently contains thirteen species (Table 1), of which only k esterite, ferrok esterite, and pirquitasite are known to display space group $\bar{I}4$. Synthetic sulfides with stannite type structures are utilized as the light absorber layer in photovoltaic cells (*e.g.* Salom  *et al.* 2012, Sasamura *et al.* 2012, Tsuji *et al.* 2010).

Pirquitasite was first described by Johan and Picot (1982), from the Pirquitas deposit, Argentina, as a silver zinc tin sulfide with ideal chemical formula $\text{Ag}_2\text{ZnSnS}_4$ and a stannite-like structure. An extensive solid solution between hocartite ($\text{Ag}_2\text{FeSnS}_4$) and pirquitasite was described by Johan and Picot (1982). Because of the solid solution and the $\bar{I}4_2m$ symmetry attributed to hocartite, Johan and Picot (1982) proposed that pirquitasite also exhibits $\bar{I}4_2m$ symmetry.

The structure was refined using both $\bar{I}4_2m$ and $\bar{I}4$, with the *R* factor for $\bar{I}4$ (*R* = 0.027) significantly lower than for $\bar{I}4_2m$ (*R* = 0.051). The structure of pirquitasite is a derivative of the cubic sphalerite structure that displays cubic closest packed (CCP) layers of S stacked along [111]. Because pirquitasite has a doubled *c* cell dimension, its stacking direction is [221]. Half of the tetrahedral sites are occupied by Ag, (Zn,Fe), and Sn cations, forming metal layers described by Hall *et al.* (1978), and it is the arrangement of Ag, (Zn,Fe), and Sn within these layers that differentiates the $\bar{I}4$ k esterite structure from the $\bar{I}4_2m$ stannite structure.

Stannite and k esterite were originally recognized as distinct species because of different Fe—Zn compositional ratios and different optical properties (Orlova, 1956; Hall *et al.* 1978). Structural and chemical analyses by Hall *et al.* (1978) and Kissin and Owens (1979) not only showed a miscibility gap between the pure Fe end-member stannite and the pure Zn end-member k esterite, but found the two minerals differed in symmetry from $\bar{I}4_2m$ (stannite) to $\bar{I}4$ (k esterite). In $\bar{I}4_2m$, Cu atoms are ordered to the Wyckoff 4*d* site, (Fe,Zn) atoms are ordered to Wyckoff 2*a*, Sn is ordered to 2*b* (Hall *et al.* 1978). For comparison, the $\bar{I}4$ symmetry has Cu atoms ordered to two sites: 2*a* and 2*c*, (Zn,Fe) ordered to 2*d*, Sn ordered to 2*b* (Hall *et al.* 1978). As pointed out by Hall *et al.* (1978), two distinct metal layers perpendicular to [001] result from this ordering in each mineral. Stannite exhibits one layer of Cu atoms only, with the other layer consisting of ordered Fe and Sn atoms, while k esterite exhibits one layer of ordered Cu and Sn atoms and one layer of ordered Zn and Cu atoms (Hall *et al.* 1978). This is illustrated for pirquitasite *versus* stannite in Fig. 1, which shows the pirquitasite structure (Fig. 1a) with one layer containing ordered Ag and Sn, the second containing ordered Zn and Ag. For comparison, the two stannite metal layers consist of one layer of Fe and Sn atoms and a second layer containing only Cu atoms (Fig. 1 b). The Ag—Sn layers in pirquitasite and Fe—Sn layers in stannite are ordered identically: Ag—Sn—Ag—Sn and Fe—Sn—Fe—Sn respectively when viewed along (100).

The mineral hocartite (tetragonal $\text{Ag}_2\text{FeSnS}_4$) is reported to exhibit space group $\bar{I}4_2m$ (Johan and Picot, 1982), but its structure is as yet unreported. It is likely that the hocartite-pirquitasite series follows the same systematics as the stannite-k esterite series.

An interesting feature is the distortion displayed by the AgS_4 tetrahedra, with tetrahedral angle variance of 8.86° displayed by Ag1S_4 and 25.40° displayed by Ag2S_4 . *M-S* bond lengths are 2.539   and 2.497   for the Ag1S_4 and Ag2S_4 tetrahedra, respectively. As our sample contains approximately 13% apfu Cu, this Cu appears to be located in the Ag2 site because the bond lengths are smaller and the tetrahedron can accommodate the distortion. Bond valence calculations gave sums of 1.28 valence units (VU) and 1.35 VU for Ag1 and Ag2, respectively, corroborating that Cu is ordered to the Ag2 site. In a study of the mechanism of incorporation of Cu, Fe, and Zn in the stannite-k esterite series, Bonazzi *et al.* (2003) studied synthetic crystals, quenched from 1023 Kelvin, of composition $\text{Cu}_2\text{Fe}_{1-X}\text{Zn}_X\text{S}_4$ ($X = 0, 1/5, 1/2, 0.7, 0.8, 1$), which showed decreasing tetrahedral angle distortion with increasing Zn content across the stannite-k esterite compositions.

Experimental

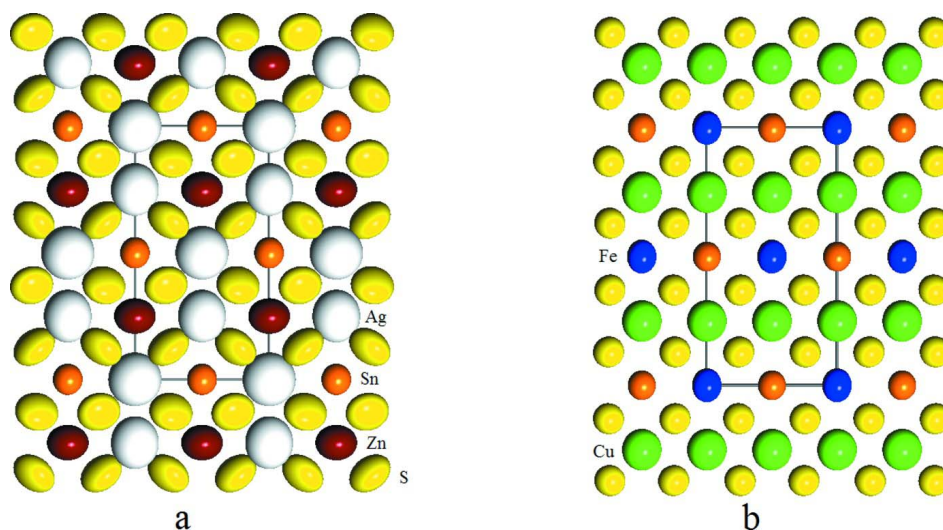
The pirquitasite specimen used in this study comes from the type locality, the Pirquitas deposit, Jujuy Province, Argentina and is in the collection of the RRUFF project (<http://rruff.info/R061016>). The chemical composition, $(\text{Ag}_{1.87}\text{Cu}_{0.13})(\text{Zn}_{0.61}\text{Fe}_{0.36}\text{Cd}_{0.03})\text{SnS}_4$, was determined with a CAMECA SX100 electron microprobe. The composition was normalized to four cations.

Refinement

The structure was refined with the inversion twin (-1 0 0/0 - 1 0/0 0 - 1) to a ratio of 0.91 (6). During refinement, the chemistry was constrained to the empirical formula of $(\text{Ag}_{1.87}\text{Cu}_{0.13})(\text{Zn}_{0.61}\text{Fe}_{0.36}\text{Cd}_{0.03})\text{SnS}_4$. The maximum residual electron density in the difference Fourier maps was located at (0.0434, 0.0434, 0.2204), 0.56   from Ag2 and the minimum at (0, 0, 0.0693) 0.75   from Ag1.

Computing details

Data collection: *APEX2* (Bruker, 2004); cell refinement: *SAINTE* (Bruker, 2004); data reduction: *SAINTE* (Bruker, 2004); program(s) used to solve structure: *SHELXS97* (Sheldrick, 2008); program(s) used to refine structure: *SHELXL97* (Sheldrick, 2008); molecular graphics: XtalDraw (Downs & Hall-Wallace, 2003); software used to prepare material for publication: *pubCIF* (Westrip, 2010).


Figure 1

Diagrams of displacement ellipsoids drawn at the 99.999% level for (a) pirquitasite and (b) stannite viewed along (100), with [001] vertical. The two types of metal layers are stacked along [001].

Disilver zinc tin tetrasulfide

Crystal data

$(\text{Ag}_{1.87}\text{Cu}_{0.13})(\text{Zn}_{0.61}\text{Fe}_{0.36}\text{Cd}_{0.03})\text{SnS}_4$

$M_r = 520.26$

Tetragonal, $I\bar{4}$

Hall symbol: I -4

$a = 5.7757$ (12) Å

$c = 10.870$ (2) Å

$V = 362.60$ (13) Å³

$Z = 2$

$F(000) = 470$

Data collection

Bruker APEXII CCD area-detector
diffractometer

Radiation source: fine-focus sealed tube

Graphite monochromator

φ and ω scan

Absorption correction: multi-scan

(*SADABS*; Sheldrick, 2005)

$T_{\min} = 0.572$, $T_{\max} = 0.633$

$D_x = 4.765$ Mg m⁻³

Mo $K\alpha$ radiation, $\lambda = 0.71073$ Å

Cell parameters from 527 reflections

$\theta = 6.3$ – 32.3°

$\mu = 12.58$ mm⁻¹

$T = 293$ K

Cuboid, grey

$0.05 \times 0.05 \times 0.04$ mm

1312 measured reflections

575 independent reflections

570 reflections with $I > 2\sigma(I)$

$R_{\text{int}} = 0.013$

$\theta_{\max} = 32.0^\circ$, $\theta_{\min} = 3.8^\circ$

$h = -4 \rightarrow 8$

$k = -8 \rightarrow 7$

$l = -16 \rightarrow 12$

Refinement

Refinement on F^2

Least-squares matrix: full

$R[F^2 > 2\sigma(F^2)] = 0.027$

$wR(F^2) = 0.070$

$S = 1.17$

575 reflections

24 parameters

4 restraints

Primary atom site location: structure-invariant
direct methods

Secondary atom site location: difference Fourier
map

$w = 1/[\sigma^2(F_o^2) + (0.0272P)^2 + 2.1498P]$

where $P = (F_o^2 + 2F_c^2)/3$

$(\Delta/\sigma)_{\max} < 0.001$

$\Delta\rho_{\max} = 1.05$ e Å⁻³

$\Delta\rho_{\min} = -0.87$ e Å⁻³

Extinction correction: *SHELXL*,
 $F_c^* = kFc[1 + 0.001xFc^2\lambda^3/\sin(2\theta)]^{-1/4}$
 Extinction coefficient: 0.0061 (6)

Absolute structure: Flack (1983)
 Flack parameter: 0.91 (6)

Special details

Geometry. All e.s.d.'s (except the e.s.d. in the dihedral angle between two l.s. planes) are estimated using the full covariance matrix. The cell e.s.d.'s are taken into account individually in the estimation of e.s.d.'s in distances, angles and torsion angles; correlations between e.s.d.'s in cell parameters are only used when they are defined by crystal symmetry. An approximate (isotropic) treatment of cell e.s.d.'s is used for estimating e.s.d.'s involving l.s. planes.

Refinement. Refinement of F^2 against ALL reflections. The weighted R -factor wR and goodness of fit S are based on F^2 , conventional R -factors R are based on F , with F set to zero for negative F^2 . The threshold expression of $F^2 > \sigma(F^2)$ is used only for calculating R -factors(gt) *etc.* and is not relevant to the choice of reflections for refinement. R -factors based on F^2 are statistically about twice as large as those based on F , and R -factors based on ALL data will be even larger.

Fractional atomic coordinates and isotropic or equivalent isotropic displacement parameters (\AA^2)

	<i>x</i>	<i>y</i>	<i>z</i>	$U_{\text{iso}}^*/U_{\text{eq}}$	Occ. (<1)
Ag1	0.0000	0.0000	0.0000	0.0364 (4)	
Ag2	0.0000	0.5000	0.2500	0.0301 (6)	0.87
Cu	0.0000	0.5000	0.2500	0.0301 (6)	0.13
Zn	0.5000	0.0000	0.2500	0.0220 (6)	0.61
Fe	0.5000	0.0000	0.2500	0.0220 (6)	0.36
Cd	0.5000	0.0000	0.2500	0.0220 (6)	0.03
Sn	0.5000	0.5000	0.0000	0.01176 (18)	
S	0.7325 (3)	0.2526 (4)	0.12847 (11)	0.0214 (3)	

Atomic displacement parameters (\AA^2)

	U^{11}	U^{22}	U^{33}	U^{12}	U^{13}	U^{23}
Ag1	0.0360 (5)	0.0360 (5)	0.0372 (4)	0.000	0.000	0.000
Ag2	0.0274 (7)	0.0274 (7)	0.0355 (9)	0.000	0.000	0.000
Cu	0.0274 (7)	0.0274 (7)	0.0355 (9)	0.000	0.000	0.000
Zn	0.0248 (8)	0.0248 (8)	0.0163 (9)	0.000	0.000	0.000
Fe	0.0248 (8)	0.0248 (8)	0.0163 (9)	0.000	0.000	0.000
Cd	0.0248 (8)	0.0248 (8)	0.0163 (9)	0.000	0.000	0.000
Sn	0.0114 (2)	0.0114 (2)	0.0125 (3)	0.000	0.000	0.000
S	0.0250 (6)	0.0212 (6)	0.0181 (6)	0.0053 (5)	-0.0023 (5)	0.0044 (5)

Geometric parameters (\AA , $^\circ$)

Ag1—S ⁱ	2.5430 (17)	Zn—S ^{iv}	2.383 (2)
Ag1—S ⁱⁱ	2.5430 (17)	Zn—S ^{viii}	2.383 (2)
Ag1—S ⁱⁱⁱ	2.5430 (17)	Zn—S	2.383 (2)
Ag1—S ^{iv}	2.5430 (17)	Zn—S ^{vii}	2.383 (2)
Ag2—S ⁱⁱⁱ	2.485 (2)	Sn—S ⁱⁱ	2.4070 (16)
Ag2—S ^v	2.485 (2)	Sn—S	2.4070 (16)
Ag2—S ^{vi}	2.485 (2)	Sn—S ^v	2.4070 (16)
Ag2—S ^{vii}	2.485 (2)	Sn—S ^{ix}	2.4070 (16)
S ⁱ —Ag1—S ⁱⁱ	113.39 (6)	S ^{iv} —Zn—S ^{viii}	107.90 (4)
S ⁱ —Ag1—S ⁱⁱⁱ	107.55 (3)	S ^{iv} —Zn—S	112.66 (8)

S ⁱⁱ —Ag1—S ⁱⁱⁱ	107.55 (3)	S ^{viii} —Zn—S	107.90 (4)
S ⁱ —Ag1—S ^{iv}	107.55 (3)	S ^{iv} —Zn—S ^{vii}	107.90 (4)
S ⁱⁱ —Ag1—S ^{iv}	107.55 (3)	S ^{viii} —Zn—S ^{vii}	112.66 (8)
S ⁱⁱⁱ —Ag1—S ^{iv}	113.39 (6)	S—Zn—S ^{vii}	107.90 (4)
S ⁱⁱⁱ —Ag2—S ^v	115.77 (7)	S ⁱⁱ —Sn—S	109.67 (4)
S ⁱⁱⁱ —Ag2—S ^{vi}	106.42 (3)	S ⁱⁱ —Sn—S ^v	109.67 (4)
S ^v —Ag2—S ^{vi}	106.42 (3)	S—Sn—S ^v	109.08 (7)
S ⁱⁱⁱ —Ag2—S ^{vii}	106.42 (3)	S ⁱⁱ —Sn—S ^{ix}	109.08 (7)
S ^v —Ag2—S ^{vii}	106.42 (3)	S—Sn—S ^{ix}	109.67 (4)
S ^{vi} —Ag2—S ^{vii}	115.77 (7)	S ^v —Sn—S ^{ix}	109.67 (4)

Symmetry codes: (i) $-y, x-1, -z$; (ii) $y, -x+1, -z$; (iii) $x-1, y, z$; (iv) $-x+1, -y, z$; (v) $-x+1, -y+1, z$; (vi) $y-1/2, -x+3/2, -z+1/2$; (vii) $-y+1/2, x-1/2, -z+1/2$; (viii) $y+1/2, -x+1/2, -z+1/2$; (ix) $-y+1, x, -z$.

Table 1. Minerals of the Stannite Group

Mineral	Formula	Space Group	Reference
Stannite	Cu ₂ FeSnS ₄	$I\bar{4}2m$	Hall <i>et al.</i> (1978)
Hocartite	Ag ₂ FeSnS ₄	$I\bar{4}2m$	Johan & Picot (1982)
Kuramite	Cu ₂ ¹⁺ Cu ²⁺ SnS ₄	$I\bar{4}2m$	Chen <i>et al.</i> (1998)
Černyite	Cu ₂ CdSnS ₄	$I\bar{4}2m$	Szymański (1978)
Velikite	Cu ₂ HgSnS ₄	$I\bar{4}2m$	Kaplunnik <i>et al.</i> (1977)
Famatinitite	Cu ₂ ¹⁺ Cu ²⁺ SbS ₄	$I\bar{4}2m$	Garin & Parthé (1972)
Luzonite	Cu ₂ ¹⁺ Cu ²⁺ AsS ₄	$I\bar{4}2m$	Marumo & Nowaki (1967)
Barquillite	Cu ₂ (Cd,Fe ²⁺)GeS ₄	$I\bar{4}2m$	Murciego <i>et al.</i> (1999)
Briartite	Cu ₂ FeGeS ₄	$I\bar{4}2m$	Wintenberger (1979)
Permingeatite	Cu ₂ ¹⁺ Cu ²⁺ SbSe ₄	$I\bar{4}2m$	Johan <i>et al.</i> (1971)
Kesterite	Cu ₂ ZnSnS ₄	$I\bar{4}$	Kissin & Owens (1979)
Ferrokesterite	Cu ₂ (Fe,Zn)SnS ₄	$I\bar{4}$	Kissin & Owens (1989)
Pirquitasite	Ag ₂ ZnSnS ₄	$I\bar{4}$	This study
Idaite	Cu ₂ ⁺ Cu ²⁺ FeS ₄	Unknown	Frenzel (1959)